Available online at www.sciencedirect.com
SCIENCE DIRECT®
Nuclear Instruments and Methods in Physics Research A 545 (2005) 319–329
NUCLEAR INSTRUMENTS & METHODS IN PHYSICS RESEARCH Section A
www.elsevier.com/locate/nima

Time-of-flight diffraction with multiple pulse overlap. Part I: The concept

U. Stuhr*

Paul Scherrer Institut, Spallation Source Division, CH-5232 Villigen PSI, Switzerland

Received 9 November 2004; received in revised form 21 January 2005; accepted 21 January 2005
Available online 19 March 2005

Abstract

The concept of a novel type of time-of-flight diffractometer for continuous neutron sources is presented. The method is based on multiple overlapping neutron pulses and allows a tuning of the instrument to high intensity and high resolution simultaneously. The dependence of the time of flight of the neutrons on the scattering angle in combination with the different intervals between successive neutron pulses are used as extra parameters for the analysis of the frame-overlap data. The instrument concept is most suitable for strain-scanning applications where high resolution in lattice spacing is necessary although the total number of Bragg reflections is quite low.

PACS: 61.12.Cd; 07.10.Pz

Keywords: Time-of-flight diffractometer; Residual stress; Strain scanner

1. Introduction

There is a growing interest for engineering and industrial applications of neutron beams. Residual stress determination by strain-field measurements is among the most important ones. In consequence, in the last decade at most neutron facilities special diffractometers for strain scanning were built or existing instruments were modified to serve this purpose.

The main requirements of strain-scanning diffractometers, high intensity and high resolution, are quite similar to that of powder diffractometers used for structure analysis. Therefore, it is not astonishing that the basic concepts of powder diffractometers have also been used for strain scanners. The desired information (strain and stress) is, however, dependent on the position and the direction within the sample. Therefore, the two major additional requirements for a strain scanner are good spatial resolution and a scattering angle 2θ close to 90°. The latter is important because the gauge volumes should have the shape

*Tel.: +41 56 310 4513; fax: +41 56 310 3131.
E-mail address: u.stuhr@psi.ch.

0168-9002/$ - see front matter © 2005 Elsevier B.V. All rights reserved.
doi:10.1016/j.nima.2005.01.320

of a cube or at least a square in the scattering plane, since only for these geometries perpendicular strain directions of the identical stress state are measured within the same volume, a necessary requirement for a correct calculation of the stress.

A simplification compared to structure analysis is, however, that typical engineering specimens show only few Bragg reflections compared to samples nowadays preferentially investigated on powder diffractometers. This will be an important argument to develop a special type of instrument for strain scanning. A further difference is that the most important information for strain scanning is the peak position, whereas for structure analysis this is the intensity of the Bragg reflections. Hence, looking into details, the requirements and conditions of strain-scanning and structure analysis are somewhat different. The present instrument concepts have not been developed for these special demands, and the question arises whether an instrument concept can be realized which better fulfills these requirements for a strain scanner.

At continuous neutron sources, the classical two-axis diffractometer is most common for strain scanning. However, there are some advantages of time of flight (TOF) diffractometers, which make this type of instrument attractive also for continuous sources. The most important advantage is that a complete diffraction pattern can be acquired at any scattering angle. Therefore, although the scattering angle can be restricted to a region close to 90°, we obtain the complete structural information of the sample. A further advantage is that the range of scattering angles 2θ can be selected. For typical strain-field measurements, a 2θ range of about 30° will be acceptable. The use of an optimized, not to narrow, 2θ range increases the intensity, since for each reflection a larger wavelength band contributes to the data.

At present two different types of TOF diffractometers are used for strain scanning: (i) conventional TOF instruments use separate pulses, i.e. the time between successive pulses must be long enough that the fastest neutrons cannot catch up with the slowest ones of the previous pulse. For each neutron, its wavelength is determined from the TOF between chopper passage and detection. The minimum time between two pulses depends on the length of the flight path and the width of the used wavelength band; typical times between pulses are some 20 ms. Strain-field measurements require high resolution for the lattice spacings, although the number of reflections is small for typical engineering samples. This leads to the situation that most of the time the detector measures only the background and not Bragg reflections. This drawback is less relevant for short-pulsed neutron sources, which is the reason why this type of diffractometer is mainly used there.

(ii) The reverse TOF- or Fourier diffractometer [1] is based on an entirely different concept. The chopper has a comb-like structure and half of the time the chopper opens the beam and half of the time the beam is blocked. Therefore, a detected neutron may have originated from several hundreds of different pulses. Only a combination of many spectra, measured at different chopper frequencies, allows the determination of the desired diffraction pattern. This type of instrument is best suited for long-pulsed sources [2], but can also be used at continuous sources [3].

About two decades ago, J.K. Cockcroft and G.J. Kearley proposed a pulse-overlap diffractometer [4] for structure analysis applications in order to enhance the intensity. In comparison to a conventional TOF diffractometer, a pulse overlap diffractometer has much shorter time intervals between the neutron pulses, and neutrons of several different pulses may arrive at the detector at the same time. The angular dependence of the TOF spectra is used as additional parameter for the analysis of the data.

In this paper, the concept of a multiple pulse-overlap TOF-diffractometer with a single chopper optimized for strain-scanning experiments is presented. It combines advantages of two-axis-, Fourier- and conventional (single-pulse) TOF diffractometers. The paper describes the concept of the diffractometer, the layout and the principles of data analysis. In the following paper, the overall performance and details of main instrument components of the strain scanner POLDI at PSI will be presented [5].

2. The basic concept

The concept of the present instrument uses a multi-slit chopper intentionally allowing multiple frame overlap. Since then the arrival time of a single neutron does not unambiguously determine its TOF, additional information is needed to evaluate the data. In the present concept, one quantity for the determination of the neutron pulse from which the neutrons came is the dependence of the TOF on the scattering angle. For that the time and angular information of the neutrons has to be recorded.

The advantage compared to a Fourier diffractometer is that the contrast within the raw data can be optimized and since no incremental variation of the chopper speed is required any duration of the measuring time can be chosen.

The TOF of a neutron between chopper and detector t_{flight} is given by

$$t_{\text{flight}} = \frac{\lambda m_{\text{n}}}{2\pi\hbar} s_{\text{tot}}(\theta), \tag{1}$$

where λ is the neutron wavelength, m_{n} is the neutron mass, $\hbar$ is Planck's constant and s_{tot} is the total length of the flight path of a neutron between chopper and detector, which may depend on the scattering angle 2θ. Eq. (1) can be combined with Bragg's law to get

$$t_{\text{flight}} = \frac{2m_{\text{n}}}{\hbar Q} s_{\text{tot}}(\theta)\sin\theta, \tag{2}$$

where $\hbar Q = 2\pi\hbar/d$ is the momentum transfer of a neutron scattered at a lattice plane with a spacing d. In a contour plot of intensity versus arrival time and the scattering angle 2θ (time–2θ plot), each Bragg reflection is represented by a line. The slopes $\mathrm{d}t/\mathrm{d}\theta$ of these lines can be expressed as a function of Q and θ, or of the TOF and θ,

$$\frac{\mathrm{d}t}{\mathrm{d}\theta} = t_{\text{flight}}\left(\cot\theta + \frac{1}{s_{\text{tot}}}\frac{\mathrm{d}s_{\text{tot}}}{\mathrm{d}\theta}\right). \tag{3}$$

This equation shows that the slope alone contains information on the TOF. Given that it is possible to calculate the TOF of the neutrons with sufficient accuracy from Eq. (3), we can trace the slit of the chopper from which the neutrons came. Knowing the exact time when this slit opened the neutron beam and the arrival times of the neutrons at the detector, the TOF of the neutrons can be calculated with the same accuracy as with a single-pulse TOF-diffractometer.

Necessary for such an analysis is a detector with time- and spatial resolution. The raw data are stored in a matrix where the elements represent the number of neutrons detected at a certain time and scattering angle.

The resolution of a TOF diffractometer comprises two components: the uncertainty in the determination of the TOF, t_{flight}, of the neutrons between the chopper and the detector and the uncertainty in the determination of the scattering angle 2θ. The uncertainty of the TOF is, for a given length of the flight path, mainly determined by the length of the neutron pulse. In a conventional TOF diffractometer, this has the consequence that an improvement of the time component of the resolution decreases the duty cycle and therefore the intensity. At a pulse-overlap diffractometer, the time component of the resolution can be tuned by the variation of the chopper speed, which does not alter the intensity but, of course, the number of overlapping pulses. As long as the intrinsic linewidth of the sample is small compared to the total resolution of the instrument, the contrast of the data remains nearly unchanged. On the other hand, if the intrinsic linewidth of the sample is relevant, a reduced chopper speed increases the contrast and therewith the quality of the data. Therefore, although the intensity does not depend on the resolution, the best performance of the instrument can be expected when the resolution is adapted to the intrinsic linewidth of the sample.

These considerations show that the two quantities, resolution and intensity, are decoupled in a pulse overlap diffractometer. The best achievable resolution for a planned instrument can be chosen by the width of the chopper slits, the total intensity by the number of slits. Within the design of the instrument, intensity and best resolution can be optimized separately. For each experiment, the optimum resolution can be selected by the chopper speed without changing the total intensity. The procedure for an optimization of the instrument

parameters will be discussed in the following two chapters.

2.1. Chopper layout

There are three chopper parameters to be optimized: the width of the slits, the number of slits and their arrangement. For a given length of the flight path and maximum chopper speed, the width of the slits defines the time component of the resolution. It should match the geometrical resolution of the instrument. In this context, it has to be pointed out that, for strain-scanning experiments, a small beam size at the chopper does not necessarily decrease the intensity at the detector. Since typically only small gauge volumes within the sample are investigated, the width of the neutron beam at the sample is also quite small. If the neutron density at the chopper position can be recovered at the sample, the width of the beam at the chopper has no influence on the measured intensity. At POLDI, for example, the conservation of the neutron density is achieved by using an elliptical neutron mirror [5].

The second parameter of the chopper is the number of slits in the chopper. A large number of slits provides a high duty cycle of the chopper and therefore also high neutron intensity. However, as discussed above, a large number of slits also increases the number of frame overlaps and therefore the number of crossings of Bragg lines in the time–2θ plot. Additionally, the regions without Bragg peaks become rare and hence the contrast gets weak. Since we want to obtain a maximum of information in a given measuring time we have to optimize intensity versus contrast. The optimum number depends unfortunately on the number of Bragg reflections of the sample. For strain-field applications, the number of Bragg peaks are typically low and high duty cycles of the chopper in the order of several per cent are favorable. More detailed information about the optimization between intensity and contrast is given in Ref. [6].

At last the distribution of the slits in the chopper can be selected. As discussed before, we also have to take care that the determination of the slopes of the Bragg lines is sufficiently accurate that each Bragg line can unambiguously be assigned to a neutron pulse. The lower limit for the repetition of neutron pulses is therefore given by the precision of the determination of the slope. Since the precision of the slope determination depends on the intensity, the linewidth and the number and position of the crossings of Bragg lines, it is favorable to push this limit into a range where it will be always fulfilled. This can be achieved by using a non-periodic slit distribution. The repetition rate of a non-periodic sequence of n_p pulses is n_p times lower compared to equally spaced slits. It is sufficient to determine the correct sequence of pulses from which the neutrons originate by the slope of the Bragg lines. The determination of which slit within the sequence corresponds to a certain Bragg line is done by comparison of the times between subsequent parallel Bragg lines with the pulse sequence. In principle, any non-periodic distribution of slits can be used within a sequence; however, it is obvious that it is favorable to use a sequence where all distances between any pairs of slits within one sequence are unique. This leads to the condition that the cross-correlation function of the slits should be flat, what is achieved best by a so-called pseudo-random distribution.

Taking all the above considerations into account, for a strain-field diffractometer, a chopper with a duty cycle in the order of several per cent is reasonable, and a resolution down to 10^{-3} is achievable with conventional techniques. In comparison with a similar conventional TOF diffractometer at a continuous source, this means that an enhancement of the intensity of up to two orders of magnitude is possible when the pulse-overlap technique is applied.

For the data analysis it is helpful, although not essential, to have a well-defined range of neutron wavelengths, since all neutron wavelengths have to be taken into account. On the long-wavelength side the Bragg edge can be used as longest wavelength, which has to be considered. On the short-wavelength side a cut-off wavelength can be achieved by neutron optics [5].

The design and requirements of the detector are closely related with the resolution of the instrument; therefore, in the next section, the detector

layout and the resolution of the instrument will be discussed.

2.2. Resolution of the total instrument and requirements for the detector

The resolution of a multiple frame-overlap diffractometer can be calculated in the same way as for any other TOF diffractometer. However, since in conventional TOF diffractometers no detector with spatial resolution is required, some special properties of such a combination has to be considered.

The resolution $\Delta Q/Q$ of a TOF diffractometer is a combination of a time component and a scattering-angle component. Assuming that there is no correlation between both, and that both have approximately Gaussian distribution, the total resolution is given by

$$\frac{\Delta Q}{Q} = \sqrt{\left(\frac{\Delta t_{\text{flight}}}{t_{\text{flight}}(Q)}\right)^2 + (\cot(\theta)\Delta\theta)^2}, \tag{4}$$

where Δ is used for FWHM of the distribution of the corresponding quantity.

The Δt_{flight} is a combination of the neutron pulse length, the time resolution of the detector and the differences in the length of the possible flight paths of the neutrons, which are mainly given by the size of the sample (or gauge volume) $2b$. The $\Delta\theta$ is given by the divergence of the incident beam α, the size of the sample, the spatial resolution of the detector Δx, and the distance between sample and detector. Position-sensitive detectors are not necessary with conventional TOF diffractometers. In this case, the detector is oriented in time-focusing geometry [7] and the thickness of the neutron absorbing volume corresponds to the spatial resolution in the above consideration. For a multiple frame-overlap diffractometer, a detector with good spatial resolution is necessary. A cell of the detector is defined by the thickness of the counting volume D, the spatial resolution Δx and its height. With a multiple wire gas detector, spatial resolutions Δx of at least 3 mm can be achieved, whereas a thickness of several centimeters is required, i.e. D is large compared to Δx. In order to avoid a large Δt_{flight} corresponding to the TOF of the neutrons through the thickness D, we have to orientate each cell of the detector such that the larger dimension of the detector cell D is aligned in the time-focusing direction. The size of D becomes then irrelevant for the resolution of the instrument. The relevant quantity is the spatial resolution Δx of the detector. The shape of a gas detector for TOF diffraction instruments will be discussed in detail in the following paper [5]. If the height of the detector and the vertical divergence of the incident beam can be neglected, the resolution of the instrument is given by

$$\frac{\Delta Q}{Q} = \sqrt{\left(\frac{\Delta t_{\text{pulse}}}{t_{\text{flight}}(Q)}\right)^2 + \left(\frac{b}{s_{\text{tot}}}\right)^2 + (\cot(\theta)\alpha)^2 + \left(\cot(\theta)\frac{b+\Delta x}{d_{\text{sd}}}\right)^2}, \tag{5}$$

which is independent of the detector thickness.

3. Data evaluation and discussion of the results

A plot of the raw data from a Ge powder sample taken at the diffractometer POLDI at PSI [5] is shown in Fig. 1. Note that the time scale is not the TOF of the neutrons, but the time elapsed since the last reset of the clock. The reset is done by an index pulse which is sent to the detector at the beginning of each sequence of neutron pulses. The complete time scale is the period of the sequences. Parallel lines in the plot correspond to identical Bragg reflections but originate from different pulses within a sequence, Bragg lines with different slopes correspond to different Bragg reflections. Despite the simple diamond-structure of the sample, the raw data alone are confusing and do not give much relevant information to the user.

The first step in data analysis is to calculate a diffractogram from the raw data, i.e. a plot of intensity versus Q or lattice spacing d, without using any a priory information about the sample. This will be done by a correlation method. In the next step, the raw data can be fitted in order to get more detailed information. The results of the correlation method are used to find an appropriate fit model (e.g. the space group of the crystal) and

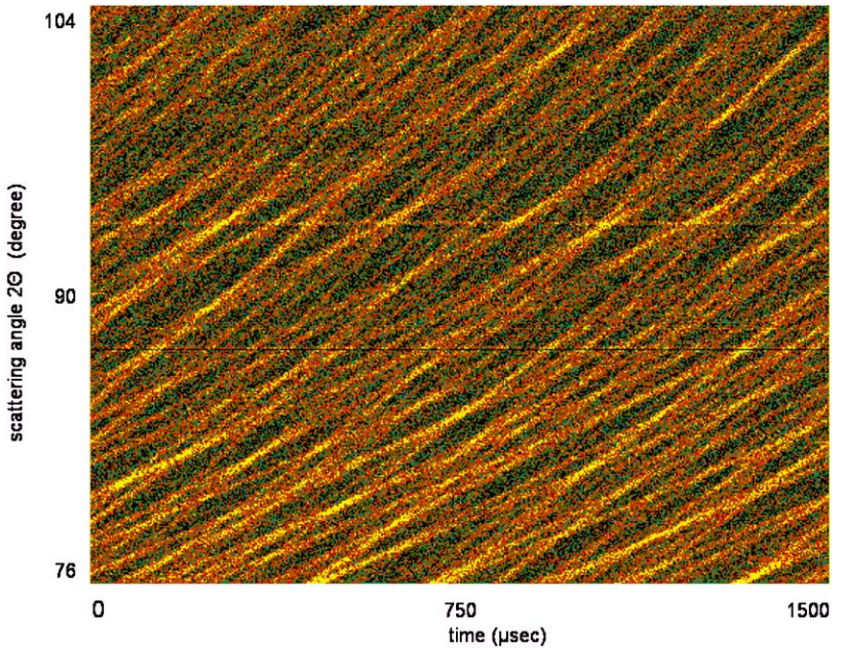

Fig. 1. Raw data of a powdered Ge sample measured on the multiple pulse-overlap diffractometer POLDI. The intensity is color encoded in this plot.

values for the initial parameters. These two methods are described in the following.

3.1. The correlation method

The principle idea for the calculation of the correlation diffraction pattern (CDP), the use of the slopes of the Bragg lines as extra parameter in order to find out which of the slits the neutrons have passed, was outlined before in the section about the basic concept of the instrument. The procedure used in the computer routine is described in the following.

At first, the TOF of neutrons scattered at an arbitrary value of the lattice spacing d, e.g. $d = 1\,\text{Å}$, is calculated for each detector cell, considering the different scattering angles and different distances of the cells from the gauge volume. The TOF corresponding to other lattice spacings are proportional to d. Next, the arrival time of the neutrons at the detector is calculated for each of the chopper slits, each detector cell, and the whole range of d. For this calculation, it must be considered that at certain positions of the chopper, always at the beginning of a new slit sequence an index pulse is sent to the detector, which resets the internal clock of the detector. The time assigned to the detected neutrons is the time between the last index pulse and the arrival of the neutron. The different neutron pulses of one sequence start at the chopper with different delays Δt_i after the index pulse. The arrival time $t_{d,i,j}$ of a neutron of neutron pulse i scattered at a lattice spacing d and detected in cell j is therefore given by

$$t_{d,i,j} = \text{tof}_{d,j} + \Delta t_i - N_{\text{index}} t_{\text{cycle}}, \tag{6}$$

where N_{index} is the number of index pulses in the interval between the start of the neutrons and their arrival at the detector and t_{cycle} is the period of the index pulses. These calculated arrival times have to be compared with the measured data. Therefore, all elements of the raw data matrix $c_{j,k}$ which coincide with the probed Bragg line are added to the intermediate correlation spectrum $I_{d,i}$,

$$I_{d,i} = \sum_j \left(k + 1 - \frac{t_{d,i,j}}{t_{\text{bin}}}\right) c_{j,k} + \left(\frac{t_{d,i,j}}{t_{\text{bin}}} - k\right) c_{j,k+1}, \tag{7}$$

where t_{bin} is the time binning and k is the integer of $t_{d,i,j}/t_{\mathrm{bin}}$.

Up to here, the procedure is similar to what is done at a Fourier diffractometer [1]. The only difference is that instead of different chopper frequencies different scattering angles are used. We look for each detected neutron if it might have been scattered with a certain Q-value; if the answer is yes we add one count at this Q-value to the spectrum.

In the next step, we consider that we have additional information of the non-periodic pulse distribution. Three qualitatively different results for a given d spacing (Q-value) are possible: (i) For a given d-value, all the values of $I_{d,i}$ are, within the statistical accuracy, the average of the whole detector intensity for all the neutron pulses i of a sequence, or (ii) the results are different for the different neutron pulses, or (iii) for all neutron pulses the intensity is higher than the average of the detector.

The conclusion from result (i) is that no Bragg reflection at this d-value contributes to the intensity. The intensity is caused by background and accidental crossings of the computed lines with Bragg lines at other d-values. Result (ii) indicates that, at the given d-spacing, there is also no Bragg reflection, since there is no justification for different intensities of different neutron pulses. However, this result can be expected when a Bragg reflection is very close to the given d-value. In such a situation, the Bragg line and the line of the probed Q-value have nearly the same slope. For one (or possibly two) of the pulses, accidentally, the arrival time of the Bragg reflection coincide with the line of the probed d-value of another pulse. However, since the distances between the pulses are all different, this coincidence cannot occur for all pulses and we can unambiguously decide whether there is a Bragg reflection or not. This is the case for result (iii). Since the distances between the Bragg lines agree with the distances between the lines of the probed d-spacing, it is now also possible to assign each of the Bragg lines to a certain neutron pulse.

There are different mathematical methods which can be applied to do this selection by a computer routine. In the present routine, the average of the reciprocal intensities of the various slits is used as expectation value of the reciprocal intensity for one pulse; the value for one point of the correlation spectrum is therefore given by

$$\mathrm{CDP}_d = n_{\mathrm{p}}^2 \left(\sum_i I_{d,i}^{-1} \right)^{-1}. \tag{8}$$

The advantage of this method is that it ascertains that whenever the intensity of at least one of the pulses is small the result also is small. This is a straightforward method and does not contain any free parameters. The disadvantage is that the performance of the method depends somewhat on the level of the background.

Since for any counted neutron many d-spacings are possible, the total intensity in the spectrum obtained by the procedure described above is much higher than the total intensity in the detector. The difference can be attributed to the so-called correlation background. This correlation background is (in the ideal case) independent of d; therefore, it can be subtracted from the CDP. However, the statistical fluctuation caused by the correlation background cannot be removed. Therefore, the statistical uncertainty at any data point of the CDP is larger than in a diffractogram of a conventional TOF diffractometer with the same intensity in the detector. Since the correlation background is d independent, the additional fluctuations are more relevant in the background and less relevant or even negligible at intense Bragg reflections. Therefore, since the pulse overlap diffractometer provides a much higher intensity than a conventional TOF diffractometer, the fluctuations at the Bragg reflections due to the correlation background are well overcompensated by the gain of intensity.

The CDP of the raw data shown in Fig. 1 is presented in Fig. 2. The correlation background has been subtracted in this figure; therefore, the total intensity is identical to the integrated intensity of Fig. 1. Between the Bragg peaks, there are pronounced fluctuations due to the correlation background. There are also dips in the background close to the strong peaks. These dips are caused by the limited range of measured scattering

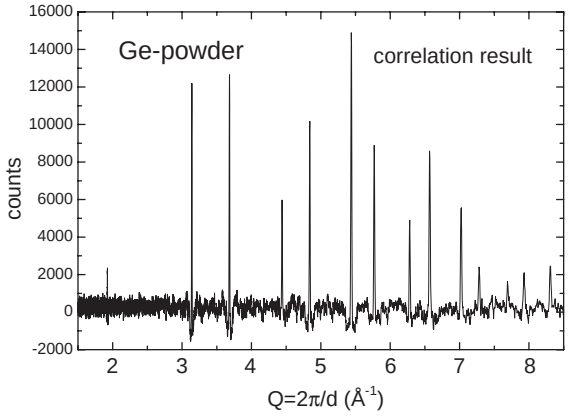

Fig. 2. Data of Fig. 1 analyzed with the correlation method.

angles 2θ. In this example, scattering angles between $\sim 76^\circ$ and $\sim 104^\circ$ were investigated. The assumption that the correlation background is Q-(d-) independent would only be fulfilled if an 'infinite' 2θ-range is measured, otherwise the contribution of the Bragg reflection close to the probed Q-value is reduced, since the corresponding line is nearly parallel to a Bragg line and does not cross it within the investigated 2θ range. Therefore, for this Q-value, the neighbored Bragg reflection does not contribute to the correlation background. At the Bragg reflection itself the contribution to the correlation background is zero. However, since for all Q-values the same correlation background was subtracted, there remains a dip. Beside this artefact, the CDP represents well the spectrum of Ge.

It has to be pointed out that for the calculation of the CDP no a priori information about the sample is necessary. The present routine also considers neither the wavelength distribution of the incident beam nor the dependence of the scattered intensity on the scattering angle. The wavelength distribution deep inside a sample cannot be computed without assumptions on the sample as well as the angular dependence of the intensity, which might be drastically influenced by absorption effects or texturing of the sample. Therefore, neglecting all these effects, which only contribute to the intensity but not to the position of the Bragg peaks, is regarded as more reliable for strain-mapping experiments, than using not well-known parameters.

The strength of the correlation method is related to the fact that the positions of the Bragg lines can be determined with high accuracy, its weakness is, as mentioned above, that the intensities of the peaks are rather a good estimate than a precise determination.

3.2. Fitting the raw data

After having applied the correlation method, it is recommended to follow with a fit to the raw data, using the results of the correlation method as initial parameters for the fit. The fit result for the data in Fig. 1 is shown in Fig. 3. The fit is based on the Levenberg–Marquart method [8], and in contrast to the correlation method it considers the angle dependence of the intensity due to the scattering cross section, the wavelength distribution and the distance from the sample to the detector. In the present example, 200,000 data points are fitted (400 angle channels $\times$ 500 time channels). This number of data points is much higher than the typical number of detected neutrons in strain-scanning experiments which are typically in the order of a few ten-thousands; therefore, the average number of neutrons per data point is much lower than 1. The fit procedure minimizes the χ^2-value, which is defined as

$$\chi^2 = N^{-1} \sum_i \frac{(n_i - f_i)^2}{\sigma_i^2}, \tag{9}$$

where N is the difference between the numbers of fitted data points and the free fitting parameters, n_i is the number of counts collected at the ith data point, σ_i is the statistical uncertainty and f_i is the value of the fit function at this data point. For a Poisson distribution σ_i is $(\tilde{n}_i)^{0.5}$, where $\tilde{n}_i$ is the expectation value of n_i. However, in general $\tilde{n}_i$ is unknown. When n_i is large enough, $\tilde{n}_i$ can be well approximated by n_i, as it is done in standard fit routines. However, in our case, n_i is small and therefore the deviations between $\tilde{n}_i$ and n_i become unacceptable, particularly since in this approximation the σ_i of all data points with n_i larger than $\tilde{n}_i$ are systematically too large and the others become

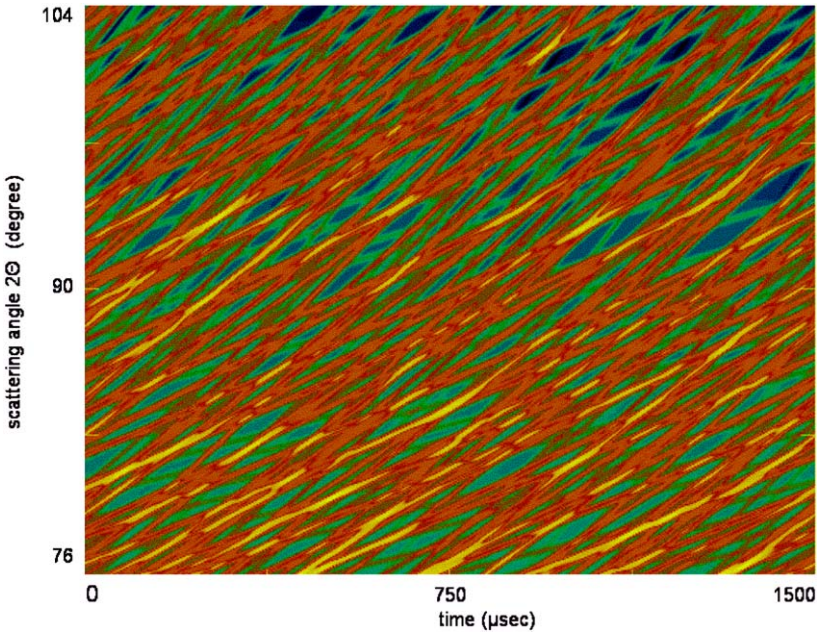

Fig. 3. Result of a fit to the raw data of Fig. 1. All reflections have been fitted individually.

too low. The consequence of this approximation is that the fitting result becomes too small. Therefore, from the point on when a fitting function, which reasonably describes the data, has been found, f_i will be a much better approximation for σ_i^2 than n_i. Therefore, in the present fitting function, σ_i^2 is approximated by n_i only in the first step and f_i is used in the following iterations. A more detailed description will be published elsewhere.

The presentation of the fit result in a time–2θ plot as in Fig. 3 makes a judgment about the quality of the fit difficult. More meaningful is the presentation as diffractogram. Whereas the fit result can easily be plotted as diffractogram this is not the case for the residuals. The residuals, the differences between Figs. 1 and 3, have to be converted. This again should preferably be done without any further assumptions. Hence, only a correlation method is applicable. The residuals can be treated with a method which is quite similar to the correlation method used for the CDP evaluation. However, the very effective method for the comparison of the intensities of different pulses has to be modified, since the intensities of the residuals might be positive or negative and are not necessarily the same for each pulse. Therefore, an iteration process has to be applied until the result has converged. This iteration routine can also be applied after the calculation of the CDP; however, it turned out that this is not necessary since no significant improvements can be achieved.

In Fig. 4, the fit result is presented as solid line, the points represent the sum of the fit and the residuals, and at the bottom of the figure the residuals are plotted separately. A comparison between Figs. 2 and 4 shows that the fluctuations in the background are drastically reduced when the fit was applied instead of the correlation method. The reason is that within the fit there are strong restrictions for the available Q-values of the Bragg reflections, whereas there is no a priori information used by the correlation method. During the fit procedure, a detected neutron on a Bragg line can be assigned only to one or a few Q-values, depending on the presence or absence of a crossing of allowed Bragg lines at this certain point in the time–2θ plot, whereas in the correlation routine it can be assigned to any Q-value, which is allowed by the instrumental configuration. The

correlation background and conclusively also the statistical uncertainties of this background is therefore reduced if a fit is applied instead of the correlation method. The dips close to the Bragg reflections have also disappeared in Fig. 4, since they are artefacts caused by the presence of strong Bragg lines, which are absent in the residuals.

In comparison to spectra measured with conventional diffractometers, a striking feature is that the fluctuations in the residuals are nearly constant, although the intensities at the Bragg peaks are a factor of up to 80 times higher than in the background. The reason is that the fluctuations are mainly caused by the Q-independent correlation background.

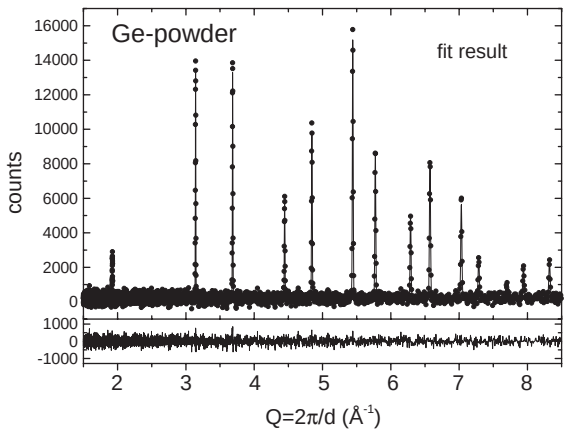

Fig. 4. The fit result of Fig. 3 converted into a diffractogram is shown as solid line. The data points are the sum of fit result plus residuals. The residuals have been calculated from the difference between Figs. 1 and 3 with a correlation method.

Table 1 shows a comparison between the fit results and the results of the correlation method. The data in the column of the correlation method are derived from fits of Gaussians to the CDP. As expected, the deviations of the results between the two methods is negligible for the peak positions whereas they are significant for the intensities.

Figs. 1 and 3 give also a good hint why the frame-overlap diffractometer might work very well for samples with low numbers of Bragg reflections in comparison to conventional diffractometers. When the data of these instruments would be presented in a similar representation, we would get a single, or few, horizontal lines for a two-axis diffractometer and 14 curved lines for a single pulse TOF-diffractometer. Note that in the latter case the time scale would be at least 10 times larger since the repetition rate is much lower. However, at both types of instruments, most of the areas would contain only background whereas in Figs. 1 and 3 at least half of the area contains intensity from Bragg reflections. Therefore, most of the additional intensity which is gained at the pulse-overlap diffractometer is accumulated in regions

Table 1
Comparison of the results for the fit and the correlation method

Miller index	Correlation method		Fit results	
	Position (Å^{-1})	Peak height (counts)	Position (Å^{-1})	Peak height (counts)
(1 1 1)	1.92372(11)	3239(274)	1.92375(6)	2530(68)
(2 2 0)	3.14103(4)	13527(145)	3.14106(3)	13475(98)
(3 1 1)	3.68318(5)	13780(174)	3.68316(4)	13399(99)
(4 0 0)	4.44166(17)	5870(186)	4.44175(10)	5860(95)
(3 3 1)	4.84028(11)	10627(193)	4.84024(7)	9876(103)
(4 2 2)	5.43965(9)	15864(198)	5.43978(6)	15153(118)
(5 1 1), (3 3 3)	5.76992(16)	9269(204)	5.76973(9)	8660(110)
(4 4 0)	6.28102(31)	5270(218)	6.28108(21)	4775(108)
(5 3 1)	6.56914(22)	8859(208)	6.56889(14)	8011(116)
(6 2 0)	7.02234(35)	5975(217)	7.02241(22)	5592(114)

The values for the correlation method are the results of a fit of Gaussian functions to the reflections in Fig. 2. The given errors are solely the statistical errors from the Gaussian fit and therefore do not include the errors introduced by transformation of the data with the correlation method.

where in conventional diffractometers only background is measured, and only a small part of this additional intensity contributes to regions with overlapping Bragg reflections.

4. Conclusion

The concept of a TOF diffractometer with multiple frame overlap has been presented, and a strategy for the optimization of the instrument parameters has been discussed. The main advantage of the concept is that the quantities resolution and intensity can be tuned independently. Therefore, it is possible to design a TOF diffractometer for continuous neutron sources with high intensity. The arrival time and the scattering angle of each neutron is determined. The dependence of the TOF on the scattering angle in combination with the different intervals between successive neutron pulses are used as extra parameters which allow the determination of the originating pulse of each Bragg line.

Two methods for data evaluation are presented. The correlation method has the advantage that no a priori information about the sample is required. This method is mainly used to get qualitative information although a precise determination of the position of the Bragg lines is well possible. The correlation background, which is inherently connected with the frame-overlap method, can be reduced when a fit is applied instead of the correlation method. The fit also gives more precise information about the intensities of the Bragg reflections. Nevertheless, for strain-field measurements, the gain of intensity, which is up to two orders of magnitude compared to conventional TOF-diffractometers, always drastically overcompensates the disadvantage of the correlation background. The method provides best benefits when high resolution is necessary although only a limited number of Bragg reflections are present. Therefore, this method seems to be ideally suited for strain-scanning experiments.

References

[1] P. Hiismäki, Neutron Inelastic Scattering, Conference Proceedings, IAEA, Vienna, 1972, p. 429.
[2] V.L. Aksenov, A.M. Balagurov, V.G. Simkin, A.P. Bulkin, V.A. Kudrjashev, V.A. Trounov, O. Antson, P. Hiismaki, A. Titta, J. Neutron Res. 5 (1997) 181.
[3] J. Schröder, V.A. Kudryashev, J.M. Keuter, H.G. Priesmeyer, J. Larsen, A. Tiitta, J. Neutron Res. 2 (1994) 129.
[4] J.K. Cockcroft, G.J. Kearley, J. Appl. Crystallogr. 17 (1984) 464.
[5] U. Stuhr, H. Spitzer, J. Egger, A. Hofer, P. Rasmussen, D. Graf, A. Bollhalder, M. Schild, G. Bauer, W. Wagner, Nucl. Instr. and Meth. A, doi:10.1016/j.nima.2005.01.321.
[6] U. Stuhr, Physica B 241–243 (1998) 224.
[7] J.M. Carpenter, Nucl. Instr. and Meth. 47 (1967) 179.
[8] P.R. Bevington, Data Reduction and Error Analysis for the Physical Sciences, McGraw-Hill, New York, 1969.